Quantum Chemical Model of an S N 2 Reaction in a Microwave Field

ARTICLE *in* THE JOURNAL OF PHYSICAL CHEMISTRY A · SEPTEMBER 2002

Impact Factor: 2.69 · DOI: 10.1021/jp012643m

Quantum Chemical Model of an S_N2 Reaction in a Microwave Field

Shirzad Kalhori,*,† Boris Minaev,*,‡ Sharon Stone-Elander,*,§ and Nils Elander*,†

Department of Physics, Molecular Physics Division, Stockholm University, SCFAB, SE-106 91 Stockholm, Sweden, Department of Biotechnology, Theoretical Chemistry Division, Royal Institute of Technology, SCFAB, S-106 91 Stockholm, Sweden, and Department of Clinical Neurosciences, Section for Clinical Neurophysiology, Karolinska Pharmacy and Hospital, Karolinska Institute SE-171 76, Stockholm, Sweden

Received: July 11, 2001; In Final Form: July 19, 2002

We have studied if and how it is possible to use quantum mechanical terms to describe the interaction between reacting molecules and the electromagnetic field in a microwave-assisted reaction. A model of an S_N2 reaction was studied by DFT and HF methods. By adding solvent molecules in the form of water, it was computationally shown that several of the models of solvated reaction complexes have vibrational modes whose frequencies are close to the normally used microwave frequency of 2.45 GHz. We thus find it likely that there may exist vibrational motion in the form of hindered rotation which overlaps with this normal microwave heating frequency in turn suggesting that microwave photons may excite these vibrational modes.

1. Introduction

Reports on microwave heating in liquid-state synthetic chemistry first appeared in 1986.[1,2] This research area has since grown rapidly, and a number of reviews[3−18] can be found. The signature of microwave-enhanced chemistry is the often dramatic increase of reaction rates when compared to conventionally heated reactions. Although many reactions require days of conventional heating, microwave-assisted techniques can produce higher yields of the same product in minutes. Sometimes new reactions can also occur. These increases and/or new reaction paths have often been attributed to so-called "special" microwave effects.

Although the heat diffusion under conventional heating goes from the walls of the reaction vessel into the reacting sample, the microwave dielectric heating is internal. The hindered, electromagnetically driven motion of the molecules is converted into heat in every subvolume in the reacting sample. This implies that one can obtain very fast temperature increases locally and that superheating[19] can occur as a result. In accordance with the Arrhenius law, the superheating of solvents may, in many cases, account for the observed rate increases. Local effects such as the hot spots that have been found in reactions performed on solid support can also contribute to the observed reaction rate increases. A number of critical studies[20,21,7] have indicated that most of the proposed microwave effects can be explained as thermal at extreme conditions. For example Gedye and Wei[20] have demonstrated that the very high reaction rates characteristic of microwave-assisted reactions are due to extremely fast heating because the same results could be obtained by conventional diffusive heating with extremely fast temperature increases. Stuerga and Gaillard[21] reviewed the different hypotheses about microwave dielectric heating. Using mainly thermodynamic and simple quantum arguments, they rejected all of the proposed "special" microwave effects as purely thermal. Gabriel et al.[13] reviewed dielectric properties relevant to microwave dielectric heating. They focused on the conventional approach and described the response of the microwaves of various solutions−solvent systems including ionic solutions. The common opinion is thus that no specific microwave effects have been proven. Still many scientists who are actively working with microwave-assisted chemistry are reluctant to give up the idea of "special" effects. Although it is acknowledged that the rapid heating in microwave-assisted chemistry is one source of the fast reaction rates, the differences between product distributions found in conventional diffusive thermal heating and microwave heating are not well understood. Langa et al.[22,23] studied the regioselectivity of the cycloaddition of *N*-methylazomethineylide to C_{70} and found that the relative yields could be modified by using microwave irradiation as a source of heat. In theoretical calculations, they found that the regiochemical outcome was related to the relative energies and also to the hardness of the transition structures involved. Langa et al.[22] also reported calculations of the average polarizability. Their data show that the transition structure with the highest polarizability is the least reactive. Quantum mechanical effects may therefore exist. To examine these effects, it is essential to find reactions which are simple enough for appropriate numerical treatment and are still meaningful to study experimentally.

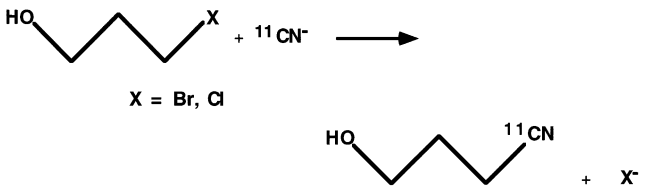

Figure 1. Example of microwave-assisted cyano-dehalogenation (from ref 24).

Some of us have previously reported an experimental study of a microwave-assisted S_N2 reaction[24] using very small molecules, which is schematically shown in Figure 1. Even this reaction is however too complicated for the model study with theoretical quantum mechanical tools as proposed here. We thus

* To whom correspondence should be addressed. E-mail: elander@physto.se. E-mail: shiri@physto.se. E-mail: boris@theochem.kth.se. E-mail: sharon.stone@ks.se.
† Stockholm University.
‡ Royal Institute of Technology.
§ Karolinska Institute.

10.1021/jp012643m CCC: $22.00
Published on Web 08/23/2002

preferred to investigate the less complicated and very often studied S_N2 model reaction:

$$Cl^-.....CH_3Cl \rightarrow \{Cl..CH_3..Cl\}^- \rightarrow ClCH_3.....Cl^- \quad (1)$$

which has the same mechanistic structure as the ones previously studied experimentally.[24]

The current understanding of microwave matter interaction and the mechanisms responsible for what is commonly known as microwave dielectric heating in liquid media are first briefly discussed in section 2. In section 3, we discuss solvation effects on S_N2 reactions in general and then how low-frequency vibrations in solvated reaction complexes may be excited by microwave radiation. Our ab initio calculations are presented in section 4. The geometry optimization of our prototype gas-phase S_N2-reaction complex as a function of the reaction coordinate is reported in 4.1. The computed permanent dipole moment and the static polarizability of the gas-phase reaction complex as a function of the reaction coordinate are presented in 4.2. Section 4 ends with a report on computationally found low-frequency torsional vibrations in models of water-solvated $(Cl-CH_3Cl)^-$ complexes. The results are discussed in section 5, whereas the conclusions are drawn in section 6. Throughout this paper we use SI units unless otherwise specified.

2. Current Understanding of Microwave−Matter Interactions

Microwaves, being electromagnetic waves in the frequency range 300 MHz to 300 GHz (wavelength range 0.1−100 cm), interact with a charge distribution through the Lorentz force:

$$\mathbf{F} = q\mathbf{E} + q\frac{\mathbf{v} \times \mathbf{B}}{c} \quad (2)$$

Here q is the charge of a single particle, **E** is the electric field, **v** is the velocity of the charged particle, and **B** is the magnetic flux density, all at the position of the particle. Only the electric component of the microwave field will take part in the energy transfer between an EM field and a charge distribution because the magnetic component Lorentz force **F** is perpendicular to the velocity of the charged particle. An ion current will be present if charges are locally present in the reacting sample. The presence of permanent and/or electric field-induced dipoles will create a polarization current when the sample is perturbed by an oscillating electromagnetic field. Two kinds of polarization are possible, as described by Stuerga and Gaillard.[21] The first has an electric charge redistribution nature which creates the induced dipoles. It shows virtually no phase difference between the applied electric field vector and the response polarization current and, accordingly, does not have any influence on the heating process. The second kind of polarization current corresponds to the hindered motion of the dipoles in the liquid or the solid substrate. Because of the size and the microscopic viscosity of the reacting medium, there will be a phase difference between the applied field and this kind of polarization current. It is generally accepted that the hindered motion of these dipoles creates microwave dielectric heating.[13,19,21,25] However, the quantum mechanical understanding of the microscopic friction is usually not presented in these studies.

The relation between the applied electric field component, **E**, and the resulting induced polarization $\mathbf{P}_{ind}$ for a given orientation of the molecules is

$$\mathbf{P}_{ind} = \alpha\epsilon_0\mathbf{E} \quad (3)$$

where α is polarizability. The sum of the permanent (μ_{0i}) and the induced dipole moment ($\alpha_{ii}E_i$) along some direction i in a molecule is then expressed as[26]

$$\langle\mu_i\rangle = \mu_{0i} + \sum_j \alpha_{ij}E_j + \text{higher terms} \quad (4)$$

The energy $\epsilon(E_i)$ of a molecule placed in an electric field $\boldsymbol{E}_i$ is given as

$$\epsilon(E_i) = \epsilon(0) - \mu_{0i}E_i - \frac{1}{2}\alpha_{ii}E_i^2 + \text{higher terms} \quad (5)$$

Taking into account that the molecules move and the electric field direction varies with time, it makes better sense to use the expression for the mean polarizability, α_{mean}, as

$$\alpha_{mean} = \frac{1}{3}\{\alpha_{xx} + \alpha_{yy} + \alpha_{zz}\} \quad (6)$$

This is more relevant for the present aim: to compare the contribution of the second and third terms in eq 5 for a realistic system. The effect of the second term in eq 5 should then be accordingly modified.

The average energy dissipated per time and volume unit, $dW_{ave}/dV\,dt$ can, by simple Ohmic reasoning,[25] be written as

$$\frac{dW_{ave}^2}{dV\,dt} = \frac{\omega}{2\epsilon_0}\mathcal{I}m(\epsilon_r)|\boldsymbol{E}_0|^2 \quad (7)$$

where ω is the angular frequency and ϵ_r is the relative dynamic electric permittivity (let $\epsilon_r = \epsilon/\epsilon_0$) of the sample exposed to an electric field. McQuarrie[27] derived the Debye−Langevin equation which relates the relative electric permittivity, temperature, polarizability, and number density of molecules, N_d, in the sample

$$\epsilon_r = \frac{1 + 2\left(\alpha + \frac{\mu_0^2}{3k_BT}\right)\frac{N_d}{3\epsilon_0}}{1 - \left(\alpha + \frac{\mu_0^2}{3k_BT}\right)\frac{N_d}{3\epsilon_0}} \quad (8)$$

Following Stuerga and Gaillard,[21] this equation can be generalized to include lossy material and will then be

$$\epsilon_r = \frac{1 + 2\left(\alpha + \frac{\mu_0^2}{3k_B\,T(1 + \iota\omega\tau')}\right)\frac{N_d}{3\epsilon_0}}{1 - \left(\alpha + \frac{\mu_0^2}{3k_B\,T(1 + \iota\omega\tau')}\right)\frac{N_d}{3\epsilon_0}} \quad (9)$$

where τ' is the microscopic relaxation time that depends on the average resistive force experienced by the individual molecules.[21] The relaxation time is defined as the time it takes for polar molecules which are aligned in a static electric field to reorient to a random directional distribution. This quantity is one of the basic parameters discussed in ref 13. Debye[28] relates the relaxation time in a system to the microscopic viscosity. This quantity, as we see it, is related to the intermolecular forces. These ideas were also touched on in ref 13. Equation 7 can be used to describe the low-frequency bands of water in the region 1−100 GHz[29] through the angular frequency ($\omega = 2\pi\nu$) variation of $\mathcal{I}m(\epsilon_r(\omega))$. Following Buchner et al.,[29] one can even model this variation by Debye theory.[21,28] However, no

first principle quantum mechanical explanation for this model[21,28] has yet appeared in the literature.

3. Don't Neglect Solvation

Stuerga and Gaillard[21] correctly pointed out important differences between microwave absorption in gas and in liquid or solid phase. However, they mainly focused on the action of the microwave field on single molecules, whether solutes or solvents, and did not consider the changing response properties of solvation complexes along a reaction coordinate.

The first statement taken from Stuerga and Gaillard[21] is that the number of collisions experienced by a given molecule and its neighbors in liquid or solid phase is of the order of 10^{15} per second, whereas there are between 10^9 and 10^{13} vibrational or rotational cycles per second. Using this, they conclude that, although the rovibrational gas-phase spectra for larger molecules do contain eigenfrequencies in the same frequency range as the common household magnetron, i.e., around 2.45 GHz,[30] a molecule in the liquid phase may not be able to complete a rotation or even a vibration before this cyclic movement is perturbed. Stuerga and Gaillard[21] also remind us that "the energy of the microwave photon is too low compared to chemical bond energies, and no breaking of chemical bonds can be induced by the absorption of one microwave photon".

Let us for a while ignore microwave irradiation and just consider the effects of solvents on any chemical reaction and on S_N2 reactions in particular. It is well-known that the solvent molecules interact with the reacting molecules. In 1969, Parker[31] stressed the influence of polar solvents on S_N2 reactions. Asubiojo and Braumann[32] compared, from a combined experimental and theoretical study, the rates of ionic nucleophilic displacement reactions and noted that these rates are many orders of magnitude faster in gas-phase reactions than in solution. Bergsma et al.[33] and Gertner et al.[34] both reported molecular dynamics calculations on the $(Cl-CH_3Cl)^-$ reaction complex solvated in water. They concluded that the reaction outcome in water is highly dependent on the local configuration of the solvent at the transition state geometry of the reaction complex. Amovilli et al.[35] presented studies of the Menshutkins reaction, which is also a simple few-atom S_N2 reaction. They noted that, although this reaction is very unfavorable in the gas-phase, polar solvents such as water facilitate charge transfer and increase the dipole moment so as to gain favorable free energies.

It is therefore clear that, when considering an S_N2 reaction in a solvent, one cannot neglect solvation shells. The reactants, the pure reaction complexes [such as $(Cl-CH_3Cl)^-$] and the product will all form larger solvated reaction complexes which will have different dipole moments and polarizabilities than the corresponding separate gas-phase systems.

Thus, because (1) larger molecules may in some cases absorb electromagnetic radiation below 10 GHz[30] and (2) dissolved molecules are known to be surrounded by solvation shells of solvent molecules,[37,38] a study of the geometry and response properties of solvation complexes is motivated.

4. Ab Initio Model Studies

4.1. Our Test Reaction: A Bimolecular Nucleophilic Displacement Reaction with Halide Ions and Halomethane. To model the suggested effects, we first considered the prototype S_N2 reaction in the gas phase

$$Cl_a^- + CH_3Cl_b \rightarrow \{Cl_a...CH_3...Cl_b\}^- \rightarrow Cl_aCH_3 + Cl_b^- \quad (10)$$

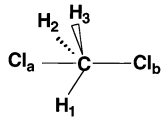

Figure 2. Schematic geometry of the reaction complex $Cl^-..CH_3Cl$. The chlorine ion that is free in the entrance channel is denoted as Cl_a, whereas the bound chlorine atom is denoted Cl_b.

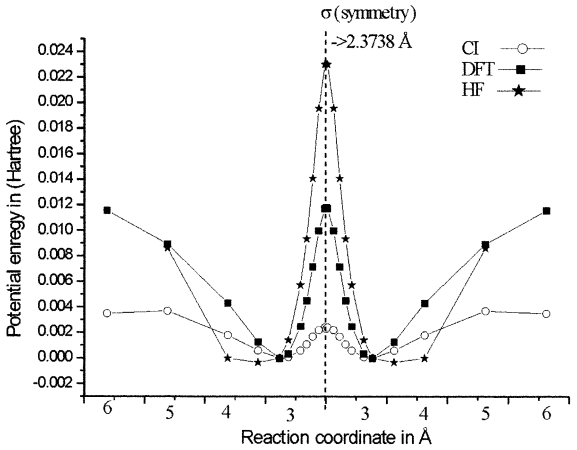

Figure 3. Cut along the reaction coordinate of potential energy surfaces for the Hartree−Fock (filled triangles), the density functional (filled circles), and quadratic single and double CI (filled squares) calculations as described in the text. The abscissa is the reaction coordinate which is defined as the distance between Cl_a and the carbon atom (R_{Cl_a-C}). The symmetry around the transition state geometry is discussed in the text.

This system has been studied by several authors which has been summarized in Shaik et al.[43] In the gas-phase, this reaction proceeds via a double well potential energy surface which has two minima separated by a central energy barrier. Both these minima correspond to ion−dipole complexes which occur at the van der Waals separation $R_{(Cl_a-C)} = 2.38$ Å.

We apply density functional theory (DFT) for structure and dipole moment calculations using the Gaussian 94[41] code, whereas the polarizability calculations were performed with the Dalton[42] package in Hartree−Fock (HF) mode. All sets of calculations have been performed with the 6−311*G** basis set (see the reference manual[41]). Geometry optimization including the reaction coordinate optimization has been performed by DFT with the B3LYP-type functional. The $^{35}Cl^-$ isotope was used in all sets of calculations. The two chlorine atoms are denoted Cl_a and Cl_b as in Figure 2 which also is used to define the notations for distances and angles. The symmetry in the reaction changes from C_{3v} in entrance to D_{3h} in transition state, C_s in all intermediate points, and finally C_{3v} in the exit channel.

The reaction coordinate is defined as the distance between the attacking chlorine ion (Cl_a^-) and the carbon atom. The *y* axis in the coordinate system coincides with the reaction coordinate. The surface of the gas-phase phase reaction is symmetric around the transition state geometry. In the calculations, the energy along the reaction coordinate has been obtained by keeping the distance between the Cl^- ion and the methyl chloride molecule frozen but varied in steps while all other bonds and angles are free to vary during the geometry optimization. The geometrical parameters of the extreme points (ion−dipole complexes and the transition state) found are very similar to those obtained from HF calculations in previous studies.[39,40]

To understand the difference between our HF and DFT results appearing in Figure 3, we also computed the potential energy

TABLE 1: Reactants $Cl^- + CH_3Cl$

	A	B	C
R_a	∞	6	
R_b	1.79	1.82	
R_{HC}	1.08	1.09	
ϕ_b	108.45	108.32	
θ	110.47	110.60	
energy (kcal/mol)	0	0	0

TABLE 2: Complex $Cl^- - CH_3Cl$

	A	B	C
R_a	3.32	3.14	
R_b	1.82	1.87	
R_{HC}	1.07	1.08	
ϕ_b	108.24	108.75	
θ	110.67	110.13	
energy (kcal/mol)	−10.28	−8.16	−9.06

TABLE 3: Central Barrier $Cl-CH_3Cl^-$

	A[a]	B[b]	C[c]
R_a	2.39	2.37	
R_b	2.39	2.37	
R_{CH}	1.06	1.07	
ϕ	90	90	
θ	120	120	
energy (kcal/mol)	3.53	−0.767	5.41

[a] Mann, D. J.; Hase, W. L. *J. Phys. Chem. A* **1998**, *102*, 6208−6214. [b] DFT calculation using B3LYP/6-311G* basis sets. [c] HF calculation using 6-311G* basis sets.

curve of the $(Cl-CH_3Cl)^-$ complex along the reaction coordinate using the Quadratic Single and Double CI (QCISD) option of Gaussian 94.[41] These results are also displayed in Figure 3. The results for three different geometries are presented in Tables 1−3. The different potential energy surfaces are energy shifted to have coinciding minima. Our results are in agreement with the statements in Shaik et al.[43] that DFT methods overestimate the stability of reagents in the S_N2 reactions and underestimate the height of the barrier. The problems associated with the use of DFT methods for chemical reactions, such as the present one, have recently been addressed by Cossi el al.[44] using the mPW1PW functional yielding results in agreement with experiments[45,46] both on the isolated molecular complex as well as for its aqueous solution. Understanding the origin of and the differences between our three potential energy curve calculations and realizing that the geometry of the obtained minima and maxima agree internally as well as with the results of other more sophisticated methods, we feel safe to use our results in the following discussion.

4.2. Permanent and Induced Dipole Moments. Equations 7 and 8 contain the permanent dipole moment as well as the polarizability. We have thus studied these two quantities. The permanent dipole moment was calculated as a function of the reaction coordinate for the gas-phase $(Cl-CH_3Cl)^-$ complex using the DFT option of Gaussian 94.[41] The results are displayed in Figure 4. We note that the complex has large dipole moments for large and small values of the reaction coordinate. The largest calculated value of the dipole moment is 25 D = 83×10^{-30} Cm.

The polarizability tensor of the ground state $|0\rangle$ is determined by[26]

$$\alpha_{\hat{i}\hat{j}} = -2\sum_n \frac{\langle 0|e\hat{i}|n\rangle \langle n|e\hat{j}|0\rangle}{E_n - E_0}, \quad \begin{cases} \hat{i} = x, y, z \\ \hat{j} = x, y, z \end{cases} \qquad (11)$$

where E_n and $|n\rangle$ are the energy and wave function of the excited

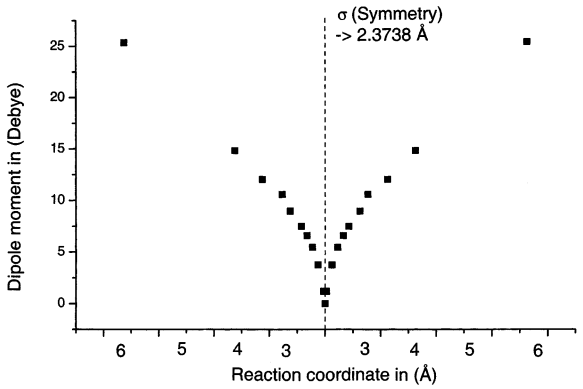

Figure 4. Permanent dipole moment for the $Cl^-..CH_3Cl$ reaction complex computed from the DFT wave functions as discussed in the text. The abscissa is the same as in Figure 3.

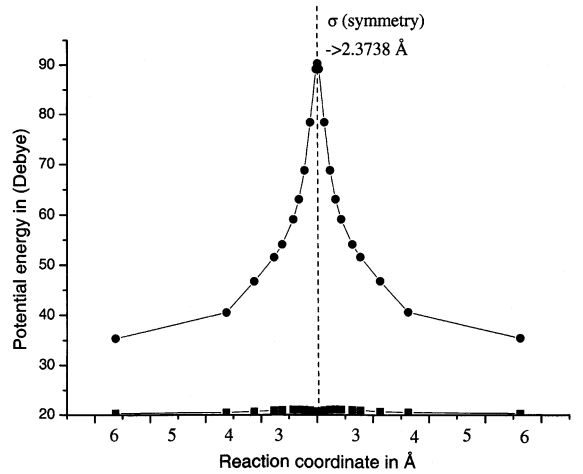

Figure 5. Parallel (filled circles) and perpendicular (filled squares) component of the static polarizability relative to the reaction coordinate for the $Cl^-..CH_3Cl$ reaction complex computed from the optimized HF wave functions as discussed in the text. The abscissa is the same as in Figure 3.

state *n*. In the transition state region, where the two adiabatic potential energy surfaces describing the reaction produce an avoided crossing, the energy gap (between them) has a pronounced minimum. At the same time, the transition dipole moments $\langle 0|\ ex\ |n\rangle$ are expected to be quite high, because the excited state *n* is connected with the charge transfer of the type

$$X^- + RY \rightarrow X^{\bullet} + RY^- \qquad (12)$$

These anticipations are completely confirmed by our response calculations.

A number of points along this reaction coordinate have been recalculated by the HF method in the polarizability calculation using the DALTON code.[42] The static polarizability components calculated by the linear response method on the HF wave functions along the reaction coordinate are presented in Figure 5. The perpendicular component is practically unchanged during the reaction. The polarizability component which is parallel to the reaction coordinate increases dramatically when the system proceeds along the reaction path. It increases from $\alpha_{||} = 34$ au for the starting reagents (this is a sum of static polarizabilities of Cl^- and methyl chloride) to 92 au at the transition state geometry. A very strong increase occurs just after the van der Waals minimum where the potential energy starts to grow and the most important chemical transformations develop. The reason we anticipate the increase of static polarizability in the

TABLE 4: Chosen Geometries, Number of Imaginary Frequencies, the Lowest Real Vibrational Frequency, and the Corresponding Intensities for Zero to Two Water Molecules[a]

		frozen							nonfrozen			
conf.	nr. H_2O	$R_{(Cl-O)}$ Å	$R_{(Cl-H_{H_2O})}$ Å	$R_{(Cl-C)}$ Å	angle ° $\angle_{Cl-C-Cl}$	ν in cm^{-1}	int km/mole	nr.im. freq.	$R_{(Cl-O)}$ Å	$R_{(Cl-H_{H_2O})}$ Å	$R_{(Cl-C)}$ Å	ν in cm^{-1}
∞				6.00	179.9	25.96	9.49					
min				3.1448	180.0	70.56	10.66					
trans				2.3738	180.0	205.09	30.19					
1	1	3.100*f*	2.282 3.032	3.000	179.4	22.143	30.95					
2	1	3.000*f*	2.226 2.864	3.100	178.4	3.718	21.72					
3	1	3.100*f*	2.284 3.030	3.100	179.8	6.3048	21.77					
4	1	3.000*f*	2.226 2.864	3.141	178.3	0.32	21.77					
5	1	3.000*f*	2.226 2.864	3.1413	178.3	0.098	21.77	2	3.17721	2.25695 3.26117	2.93962	8.751
6	2	3.39143	2.54467*f* 3.38707*f*	3.36657	179.1	0.076	0.4437	2	3.26036	2.40587 3.31498	3.36603	7.588
		3.25559	2.4000*f* 3.31312*f*							3.53779 2.72695	3.46384	

[a] The bond lengths which are frozen during the DFT geometry optimization are marked with an *f* after the bond length. All other bond lengths and angles are allowed to vary. The nonfrozen data for the same systems are displayed as a comparison.

region of the transition state is that the barrier is usually produced by the avoided crossing of two singlet states, as discussed above.

Let us now assume an electric field strength of 10^7 V/m as in ref 21. The induced dipole moment is through eq 4 obtained as 92 atomic units $= 1.5 \times 10^{-32}$ Cm. This should be compared to the maximum permanent dipole moment of 83×10^{-30} Cm. The contribution from the permanent dipole moment is thus about 6000 times larger than the contribution from the induced dipole moment. We then note that the electric field strength used is about 5000 times the electric field strength of 2×10^3 V/m which was recently simulated at our laboratory[47] using a resonance cavity with a small water load. Now turning back to eqs 6−8, we find it likely that the induced dipoles have very little effect on the microwave adsorption at least as it is described in the Debye-theory[21,28] based models.

4.3. Models of Solvated Reaction Complexes and Their Vibrational Frequencies. Solvation of the Cl^- anion by a few water molecules gives rise to a substantial decrease in the rate constant. A well-known kinetic aspect of S_N2 reactions is the smaller rate constants in aqueous solutions as compared to the corresponding gas-phase processes.[39] In solution, the importance of the two ion−dipole complexes is mitigated, and the central barrier is more dominant because of the extensive solvation of the Cl^- anions. The water molecules will further arrange themselves around the reaction complex before the reaction. During the reaction the entire ion−dipole complex will have solvation shells around it. When considering the energy absorption in a microwave-assisted reaction, one should thus not, as is done many times, consider properties such as dipole moments of the solvent or the separate reactants. Instead, it makes sense to study the response properties of the solvated reaction complexes. This point of view is in agreement with previous theories of Debye[13,21,28,29] where the absorbing molecular systems are approximated as spherical with a given dipole moment.

Several new problems have to be considered when going from gas phase to liquid phase. Results from molecular dynamics and extensive ab initio calculations give some hints on how these problems may be tackled. It is not obvious that the reaction coordinate used above in the gas-phase study appropriately describes the liquid-phase reaction. Several closely related studies are to be found in the literature. Water solvation effects on this model S_N2 reaction were studied by Ensing et al.[49] Steric effects in S_N2 reactions and the influence of microsolvation were studied by Mohamed and Jensen.[50] Nonequilibrium effects in solvation on chemical rates for the microsolvated $Cl^-(H_2O)_n...CH_3Cl$ system were studied by Tucker and Truhlar.[51]

If quantum absorption plays an important role in dielectric microwave heating, a considerable number of solvated reaction complexes which possess vibrational frequencies close to or overlapping with the common magnetron frequency of 2.45 GHz must exist. Finding these is as formidable a task as the classical looking for a needle in a haystack. Therefore, only a few examples in which a few water molecules are closely positioned and interacting with the reacting $(Cl-CH_3Cl)^-$ complex are considered here. The structure of these solvated complexes are computed, using the DFT option of Gaussian 94. All calculations discussed below are made close to the gas-phase van der Waals ion−dipole complex minimum on the left-hand side of transition state geometry of the gas-phase $(Cl-CH_3Cl)^-$ system as displayed Figure 3.

The vibrational frequencies and the corresponding intensities are determined. The internal motion of the largest displacements for each such vibration is further analyzed. We thus investigate geometries in which one, then two, three, and five water molecules are surrounding the $(Cl-CH_3Cl)^-$ complex.

The first three entries in Table 4 describe geometries and low-frequency vibrations in the naked $(Cl-CH_3Cl)^-$ complex and are added to the table in order to allow comparison with the solvated complexes. The first line in the table corresponds to our approximation of an asymptotic configuration, prior to the reaction. The lowest calculated vibrational frequency is about 25 cm^{-1} with an intensity of 1 km/mol. When the attacking chlorine ion has reached the geometry of the gas-phase van der Waals ion−dipole complex minimum (see Figure 3), the lowest frequency has increased by a factor of almost three, whereas the corresponding intensity is almost unchanged. The lowest calculated frequency for transition state geometry is again another factor of 3 larger, whereas the corresponding intensity has increased by a factor of 3.

Five similar geometries including only one water molecule, as illustrated with one example in Figure 6, were studied. The

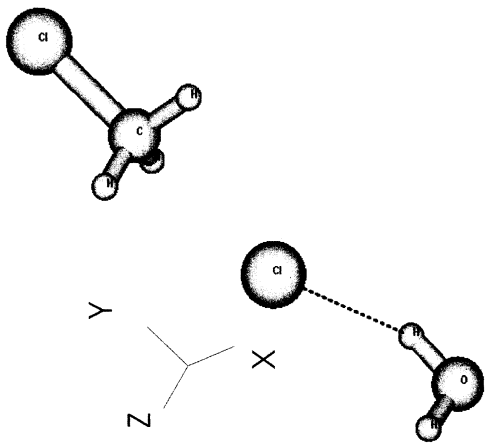

Figure 6. Geometry of the family of solvated $(Cl-CH_3Cl)^-$ complex with one water molecules, with entries 1−5 as described in Table 4. The reaction coordinate is along the *y* axis. The figure is obtained from the Gaussian 94 output by using the Molden[52] code.

oxygen of the water molecule is, by the geometry optimization, placed approximately on an axis through both chlorines and the carbon atom. The relative positions of the oxygen to the adjacent chlorine atom as well as the distance between the same chlorine atom and the carbon atom were frozen in each calculation, whereas the positions of the rest of the atoms were optimized. The calculations discussed below are all performed with the attacking Cl^-_a ion being close to the van der Waals minimum, to the left of the transition state.

Now consider the first solvated configuration in Table 4. The water molecule has a torsional frequency of 22 cm^{-1} with an intensity of 30 km/mol, whereas the CH_3 group shows conjugated torsional movement. The vibrational motion is centered around the axis which is also the reaction coordinate axis. In the second configuration, we decreased the $O-Cl_a$ distance by 0.1, whereas the $C-Cl_a$ distance was increased by 0.1. The water torsional vibrational frequency has now decreased by a factor of almost seven to 3.7 cm^{-1}, whereas the intensity is reduced by a factor of 1.5 to 22 km/mol. The same kind of conjugated torsional motion as above is found for the CH_3 group. Now we increase the Cl−O distance back to 3.1, whereas the Cl−C distance is kept at 3.1. This change results in approximately a doubling of the lowest vibrational frequency, whereas the corresponding intensity remains the same. Again reducing the Cl−O distance to 3.000 Å and increasing the Cl−C distance to 3.141 Å, we obtain a reduction of the lowest torsional intramolecular vibration to 0.32 cm^{-1}. A further slight change of the Cl−C distance gives a vibrational frequency of 0.098 cm^{-1}, whereas the intensity remains the same. Note that the fourth frequency is only a factor of 4 higher than the assumed applied microwave frequency (0.082 cm^{-1}), whereas the fifth computed frequency is only twenty percent too high. All five cases have intensities between 20 and 30 km/mol.

We have with this set of calculations shown that one solvated $H_2O...(Cl-CH_3Cl)^-$ can have low torsional vibrational frequencies in the region of interest. This situation does not correspond to the real situation, where the $(Cl-CH_3Cl)^-$ complex is surrounded by several solvation shells. To model a more realistic situation, we thus have to use geometries similar to those obtained in molecular dynamics simulations of solvated $n(H_2O)...(Cl-CH_3Cl)^-$ complexes.

Ensing et al.[49] have very recently used a combination of DFT and molecular dynamics in a study of our water solvated reaction. Using Car-Parrinello molecular dynamics simulations with 32 water molecules surrounding the $[Cl_a...CH_3-Cl_b]^-$ complex, they find that angle $\angle_{Cl_aCCl_b}$ is 176°. Our corresponding angles given in Tables 4 and 5 are close to this value. The coordinates of the solvated $[Cl_a...CH_3-Cl_b]^-$ complex in our study are in agreement with those of Ensing et al.[49] This implies that our choices of reaction coordinates for all cases are reasonable, at least just before and in the barrier region. Furthermore, Ensing et al.[49] find that the water molecules mainly create an inner solvation shell around the attacking Cl_a^- ion. The distances between the attacking Cl_a^- ion and oxygen in the water molecules in these simulations were found to be around 3.3 Å ranging from 2.9 to 3.8 Å.[49] The distance between the attacking Cl_a^- ion and the first solvation shell hydrogen atoms are around 2.3 Å ranging from 1.8 to 2.6 Å. We conclude therefore that about 3−5 water molecules create the innermost solvation shell. The relevant geometries from ref 49 are included in Table 5. From the figures in ref 49, we conclude that the second solvation shell hydrogen atoms are located in a radial shell with an average radius of 3.5−4 Å.

We have with this in mind studied solvation shells with two, three, and five water molecules surrounding the attacking Cl_a^- ion. The optimal geometries which have low resonance frequencies are presented in Tables 4 and 5 and in Figures 8−9. The results are obtained by fixing the $R_{(Cl-H_{H_2O})}$ distances, whereas all other distances are geometry optimized. For two water molecules, we find a torsional vibrational resonance at 0.076 cm^{-1}. Both oxygen atoms are within the first radial distribution maximum of ref 49. Similarly, one hydrogen atom in each water molecule has $R_{Cl-H_{H_2O}}$ within the first radial distribution shell of ref 49, whereas the other two are located between the first and the second shell maxima of ref 49.

The results of our calculations for a solvated $[Cl_a...CH_3-Cl_b]^-$ complex with three water molecules are presented in Table 5. We find all three oxygen atoms within the first radial distribution shell of ref 49. Also here half of the solvating hydrogen atoms are within the first molecular dynamics radial distribution shell,[49] whereas the three remaining hydrogens are located between the first and the second shell maxima of Ensing et al.[49]

Modeling the solvation effects with five water molecules around the attacking Cl^- ion, we find that all oxygen atoms are within the first molecular dynamics solvation shell.[49] Here, only three of the total 10 hydrogen atoms are within the innermost molecular dynamics solvation shell, two are located between the first and the second molecular dynamics solvation shells, and the remaining five hydrogen atoms seem to belong to the second molecular dynamics solvation shell of Ensing et al.[49] Two imaginary frequencies were obtained in the reported one, two, and three water molecule cases, whereas for five water molecules, we only find one such frequency. This implies that the one, two, and three water molecule cases are on a slope, whereas the five water molecule case corresponds to a saddle point. Further analysis shows that one of the water molecules is in a transition state like configuration. All cases have saddle point motions. By making just a slight change in these geometries it is possible to change the number of imaginary frequencies by one. Thus, the number of imaginary frequencies are in all cases small, as they should be in dynamic situations.

The DFT results discussed so far (the eight first columns in Tables 4 and 5) were obtained by keeping one bond length fixed while all other bond lengths and all angles were allowed to vary. These results are compared with those we obtained when all bond lengths and angles were allowed to vary (the four last columns in Tables 4 and 5). The partially frozen coordinate

TABLE 5: Chosen Geometries, Number of Imaginary Frequencies, the Lowest Real Vibrational Frequency and the Corresponding Intensities for Three and Five Water Molecules

		frozen							nonfrozen			
conf.	nr. H_2O	$R_{(Cl-O)}$ Å	$R_{(Cl-H_{H_2O})}$ Å	$R_{(Cl-C)}$ Å	angle ° $\angle_{Cl-C-Cl}$	ν in cm^{-1}	int km/mol	nr.im. freq.	$R_{(Cl-O)}$ Å	$R_{(Cl-H_{H_2O})}$ Å	$R_{(Cl-C)}$ Å	ν in cm^{-1}
7	3	3.57524	2.76332*f*	3.40220	179.2	0.0993	0.6094	2	3.57973	2.75883	3.39885	7.044
			3.51209*f*							3.53441		
		3.14924	3.35367*f*						3.21146	3.31904		
			2.21990*f*							2.31582		
		3.54810	3.49622*f*						3.55800	3.52011		
			2.73000*f*							2.73437		
8	5	3.40427	2.99713*f*	3.43553		0.09002	0.4807	1	3.4068	2.5897	3.43288	8.191
			3.68196*f*							3.49528		
		3.86813	3.32982*f*						3.8698	2.93830		
			2.23050*f*							3.32982		
		3.17749	3.68575*f*						3.6245	3.68605		
			3.52863*f*							3.57413		
		3.78705	2.93830*f*						3.2578	2.31745		
			3.48878*f*							3.7234		
		3.60855	2.58970*f*						3.80144	2.99713		
			3.49451*f*						3.54587			
–	Ensing I	2.9–3.8	1.8–2.6		176							
–	Ensing II	2.9–3.8	3.5–4.0		176							

[a] The bond lengths which are frozen during the DFT geometry optimization are marked with an *f* after the bond length. All other bond lengths and angles are allowed to vary. The nonfrozen data for the same systems are displayed as a comparison. Ensing I relates the first maximum for the radial distributions g_{Cl_a-O} and the first maximum for g_{Cl_a-H} from Figure 6 in ref 49, whereas Ensing II relates the first maximum for the radial distributions g_{Cl_a-O} and the second maximum for g_{Cl_a-H} from Figure 6 in ref 49.

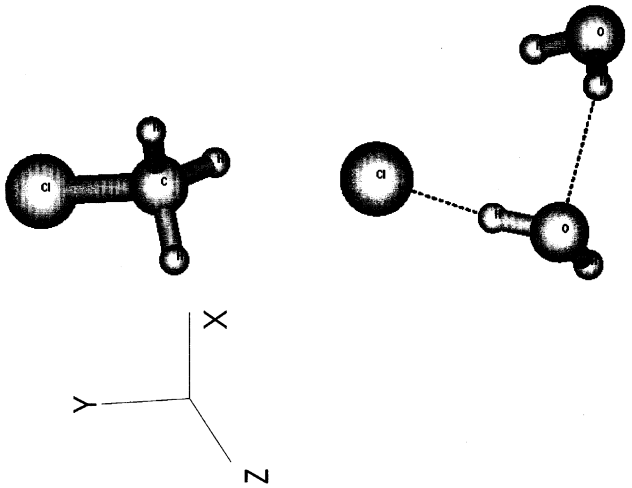

Figure 7. Geometry of the family of solvated $(Cl-CH_3Cl)^-$ with two water molecules. The reaction coordinate is along the *y* axis. The figure is obtained from the Gaussian 94 output by using the Molden[52] code.

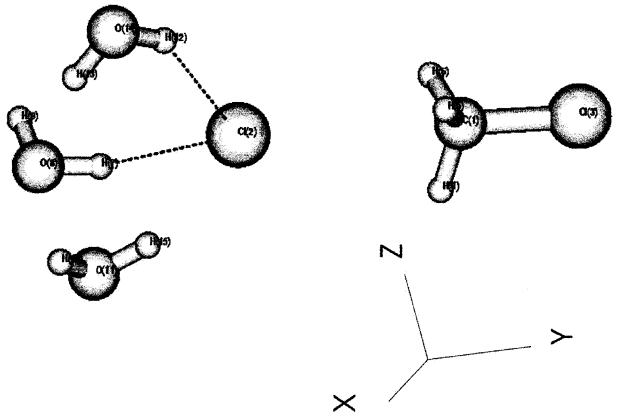

Figure 8. Geometry of the family of solvated $(Cl-CH_3Cl)^-$ complex with three water molecules. The reaction coordinate is along the *y* axis. The figure is obtained from the Gaussian 94 output by using the Molden[52] code.

studies for given $R_{(Cl-H_{H_2O})}$ distances deviate more from the corresponding low-frequency nonfrozen cases, whereas the corresponding $R_{(Cl-O)}$- and R_{Cl-C} distances show a better agreement.

Summing up, the average oxygen–chlorine distances are within the first molecular dynamics radial distribution maximum found by Ensing et al.[49] Our DFT-computed average oxygen–chlorine distances seem to increase with the number of water molecules in the solvated complex. The corresponding hydrogen atoms in our calculations are somewhat further away from the attacking chlorine ion than in the molecular dynamics study of Ensing et al.[49] However, the deviations between all four sets of calculations and the MD result are small, especially when considering that we are interested in the geometry of vibrational distributions rather than of static geometry.

To estimate the size of the vibrational distributions, we then considered the geometry distribution caused by the discussed vibrations and used the amplitudes for the five water solvation-complex as an example. We chose the low-frequency vibration at $\nu = 0.09$ cm^{-1}. The atoms which have amplitudes A_i, $i = x$, *y*, *z*, larger than 0.1 Å are listed in Table 6. The notations used are the same as in Figure 9. We observe a torsional vibration where the atoms in the water molecules described by (H7, O8, H9), (H10, O11, H12), and (H13, O14, H15) all have vibrational amplitudes between 0.1 and 0.3 Å in the *x* but also in the *y* direction.

Both the attacking and the leaving chlorine atoms (Cl_a and Cl_b respectively) have large amplitudes in the y direction. Our computed result implies therefore, that a microwave photon may excite an internal motion which promotes the motion of the Cl_a^- relative to the carbon atom. For the three-water case, we find that the attacking Cl_a ion has a vibrational motion parallel to the reaction coordinate. The results for the two-water complex are similar.

When these vibrational motions are excited by a photon, we interpret it as a direct injection of microwave energy into the system that drives the reaction from reactants to products. The motion we describe is quantum mechanical and thus gives a probability distribution for a dynamic reacting system. Using

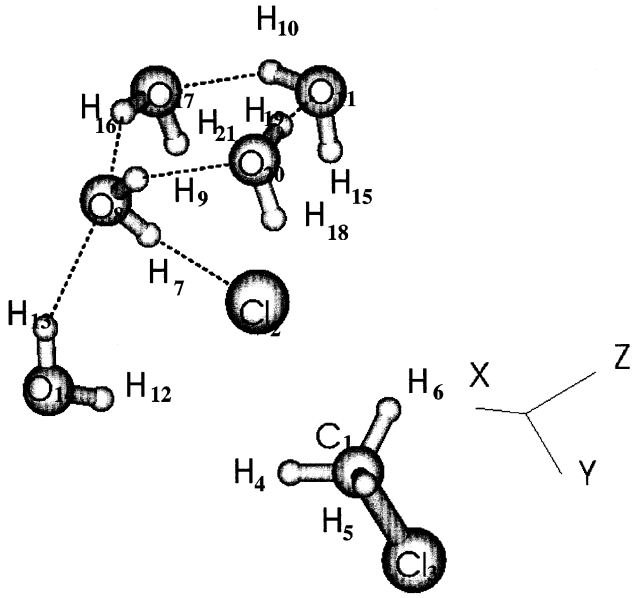

Figure 9. Geometry of the family of solvated $(Cl-CH_3Cl)^-$ complex with five water molecules. The reaction coordinate is along the *y* axis. The notation of the atoms correspond to that in Table 6 and in the text. The figure is obtained from the Gaussian 94 output by using the Molden[52] code.

TABLE 6: Torsional Vibrational Amplitudes (A_x, A_y, A_z) for the Five Water Molecule Reaction Complex at the Vibrational Frequency $\nu = 0.0908$ cm^{-1} for a Selected Set of Atoms with the Largest Amplitues[a]

atom	nr.	A_x	A_y	A_z
C	1	−0.01	0.07	0.0
Cl_a	2	−0.02	−0.30	0.02
Cl_b	3	0.0	0.25	−0.02
H	7	0.10	−0.03	−0.01
O	8	0.13	0.08	−0.02
H	9	0.11	0.11	−0.03
H	10	−0.28	0.03	0.02
O	11	−0.30	−0.03	0.03
H	12	0.31	−0.20	0.02
H	13	0.33	−0.04	−0.01
O	14	0.38	−0.13	0.01
H	15	−0.26	−0.14	0.03

[a] The number in the second column identifies the atom as in the Molden[52] generated Figure 9.

this point of view, the deviation between our results and the statistical average molecular dynamics results of Ensing et al.,[49] being within the vibrational profile limited by the amplitudes in Table 6, well motivates our assumption that microwave photons may be absorbed by a real water-solvated reaction complex.

5. Discussions

This study has addressed possible quantum mechanical effects in the interaction between the electric component of the 2.45 GHz microwave field in microwave-enhanced chemistry. A previous study of Stuerga and Gaillard[21] focused on the properties of the solvents or the reactants, whereas we have considered various models of a reaction complex.

The direct influence of the electric component of the microwave field on the reaction complex was studied first. It was found that the permanent dipole moment as well as the static polarizability have a pronounced variation along the reaction coordinate. Although the dipole moment is trivially large at geometries where the approaching or leaving chlorine ion is far from the methyl chloride molecule, the static polarizability has a maximum at the transition state geometry. We applied first the conventional approach, in which microwave dielectric power influenced the electrostatic energy of the reacting system. We therefrom find it likely that the coupling of the permanent dipole moment of the molecules with the electric component of the microwave field gives a much stronger contribution to the energy transfer from microwave electric field to the reaction than the corresponding coupling to the induced dipole moment does. This first part of our study does not give any essential new understanding of the microwave dielectric heating process.

When various models of water solvated $(Cl-CH_3Cl)^-$ reaction complexes are considered, we notice that these complexes may have absorption frequencies in the microwave energy region with one, two, three, and five water molecules in the innermost solvation shell. These resonance frequencies represent hindered rotations which involve the solvation shell water molecules. From the present set of calculations, which is by no means complete, we may conclude that suitable arrangements of polar solution molecules around the reaction complex may be able to give solvation structures (including reaction complexes) which have almost any vibrational frequency in the region of the exciting magnetron frequency of 2.45 GHz ($\Leftrightarrow \nu = 0.082$ cm^{-1}) The intensities found are comparatively high. This implies that we cannot exclude that these solvated complexes can absorb the applied microwave radiation. The cases we have found, with a rather limited search, suggest in fact that a large number of suitable solvated systems exist that are able to absorb the magnetron generated microwave radiation. Experimental microwave resonance frequencies in the relevant frequency region have also been reported.[30]

In the analysis, we find that all these liquid phase vibrations, which are actually torsional vibrations in the water molecule, are coupled to conjugated torsional vibrations of the CH_3 group. The observed vibrations may be directly involved in the energy transfer from the microwave-absorbing attached water molecule to the reaction complex close to the transition state geometry. Because the vibrations are found to depend on the geometry of the reaction complex, it is not surprising that different product distributions may be obtained when using conventional diffusive thermal heating and microwave heating. Although conventional diffusive thermal heating excites all internal molecular motions, our present results show that the microwave photon excitations are geometry specific. The observations of Langa et al.[22,23] may thus be interpreted in this way. However, a lot of systematic studies need to be done before one can be fully conclusive about the microwave vibration excitation effect proposed here. An important point is that the hindered rotation of a water molecule (which is usually present in most microwave processes in solvents) is now weakly mixed with the internal motion of CH_3 group in the reacting system at a few points studied along the reaction coordinate.

6. Conclusions

The recent study of Langa et al.[22,23] implies that microwaves may have quantum mechanical effects on chemical reactions. A model study of a reaction that is mechanistically similar to a microwave-enhanced reaction was undertaken here in order to further examine this proposal. Previous work has been briefly discussed, and it is pointed out that the relevant electromagnetic response properties of the microwave-enhanced reaction studied were those of the reaction complex. We may conclude the following:

(1) Studying the pure gas-phase reaction complex, we found that the effects of induced dipole moment on the microwave energy absorption is negligible when compared to the microwave energy absorption caused by the permanent dipole moment.

(2) A study of a reaction complex in a nongas phase environment should include solvation shells. The models of the water-solvated reaction complexes were all shown to possess low frequency vibrations or hindered rotations with frequencies overlapping that of microwave radiation typically used in microwave-enhanced chemistry.

(3) The reaction coordinates used in the present study are close to those obtained by Ensing et al.[49] Adding that (1) the spatial distribution of these vibrations overlap the reaction coordinates of Ensing et al.,[49] (2) that the intensities of the computed hindered rotations are nonnegliable, and (3) the presently found water molecule distributions agree with the solvation shells found by Ensing et al.[49] all together suggest that absorption of microwave photons may play an important role in these type of reactions.

Using the two latter points, we suggest further work in order to theoretically and experimentally verify the existence of the low-frequency hindered rotations found in this study in this and similar systems.

Acknowledgment. The research was supported by a research grant from the Swedish Technical Research Council (TFR) and a graduate student scholarship from Stockholm University. B.M. acknowledges support from the Swedish Royal Academy of Sciences. Support from Personal Chemistry AB, Uppsala, Sweden is kindly acknowledged. This work was performed under the European COST D10 program.

References and Notes

(1) Gedye, R.; Smith, F.; Westaway, K.; Ali, H.; Baldisera, L.; Laberge, L.; Rousel, J. *Tetrahedron Lett.* **1986**, *27*, 279.

(2) Giguere, R. J.; Bray, T. L.; Duncan, S. M.; Majetich, G. *Tetrahedron Lett.* **1986**, *27*, 4945.

(3) Abramovitch, R. A. *Org. Prepr. Proced. Int.* **1991**, *23*, 685.

(4) Gedye, R.; Smith, F.; Westaway, K. *J. Microwave Power Electromag. Energy* **1991**, *26*, 1.

(5) Bram, G.; Loupy, A.; Villemin, D. In *Solid Supports and Catalysts in Organic Synthesis*; Smith, K., Ed.; Ellis Horwood Ltd.: London, 1992; pp 302−326.

(6) Majetich, G.; Hicks, R. *Res. Chem. Intermed.* **1994**, *20*, 61.

(7) Strauss, C. R.; Trainor, R. W. *Aust. J. Chem.* **1995**, *48*, 1665.

(8) Caddick, S. *Tetrahedron* **1995**, *51*, 10403.

(9) Galema, S. A. *Chem. Soc. Rev.* **1997**, *26*, 233 and references therein.

(10) Langa, F.; de la Cruz, P.; de la Hoz, A.; Diez-Ortiz, A.; Diez-Barra, E. *Contemp. Org. Synth.* **1997**, *4*, 373.

(11) Kingston, H. M.; Haswell, S. J. *Microwave-Enhanced Chemistry, Fundamentals, Sample Preparation and Applications*; American Chemical Society: Washington, DC, 1997; and references therein.

(12) Loupy, A.; Petit, A.; Hamelin, J.; Texier-Boullet, F.; Jacquault, P.; Math, D. *Synth.−Stuttgart* **1998**, *9*, 1213.

(13) Gabriel, C.; Gabriel, S.; Grant, E. H.; Halstead, B. S. J.; Mingos, D.M. P. *Chem. Soc. Rev.* **1998**, *27*, 213 and references therein.

(14) Strauss, C. R. *Austr. J. Chem.* **1999**, *52*, 83.

(15) Varma, R. S. *Green Chem.* **1999**, *1*, 43.

(16) Elander, N.; Jones, J. R.; Lu, S.-Y.; Stone-Elander, S. *Chem. Soc. Rev.* **2000**, *29*, 239.

(17) Larhed, M.; Hallberg, A. *Drug Discovery Today* **2001**, *6*, 406−416.

(18) Lidström, P.; Tiernye, J.; Wathey, B.; Westman, J. *Tetrahedron* **2001**, *57*, 9225.

(19) Baghurst, D. R.; Mingos, D. M. P. *J. Chem. Soc., Chem. Commun.* **1992**, 674.

(20) Gedye, R. N.; Wei, J. B. *Can. J. Chem.* **1998**, *76*, 525.

(21) Stuerga, D. A. C.; Gaillard, P. *J. Microwave Power Electromagn. Energy* **1996**, *31*, 87; *J. Microwave Power Electromagn. Energy* **1996**, *31*, 101.

(22) Langa, F.; de la Cruz, P.; de la Hoz, A.; Espildora, E.; Cossio, F. P.; Lecea, B. *J. Org. Chem.* **2000**, *65*, 2499.

(23) Langa, F.; de la Cruz, P.; de la Hoz, A.; Espildora, E.; Cossio, F. P.; Lecea, B. *Proceedings of the International Conference on Microwave Chemistry*. Antibes -Juan-les Pins; Inst. National Polytechn. de Toulouse: Toulouse, France, 2000.

(24) Thorell, J.-O.; Stone-Elander, S.; Elander, N. *J. Labeled Comp. Radiopharm.* **1993**, *31*, 207.

(25) Collin, R. E. *Field theory of Guided Waves*, 2nd ed; McGraw-Hill: New York, 1991. Collin, R. E. *Foundations of Microwave Engineering*, 2nd ed; McGraw-Hill: New York, 1992.

(26) Atkins, P. W. *Molecular Quantum Mechanics*; Clarendon Press: Oxford, U.K., 1983.

(27) McQuarrie, D. A. *Quantum chemistry*; Oxford University Press: New York, 1983.

(28) Debye, P., Ed.; *Polar molecules*; Dover: New York, 1945; p 147.

(29) Buchner, R.; Batheland, J.; Stauber, J. *Chem. Phys. Lett.* **1999**, *306*, 57.

(30) *Modern Aspects of Microwave Spectroscopy*; Chantry, G. W., Ed.; Academic Press: London 1979.

(31) Parker, A. J. *Chem. Rev.* **1989**, *69*, 1.

(32) Absubiojo, O. I.; Braumann, J. I. *J. Am. Chem. Soc.* **1979**, *101*, 3716.

(33) Bergsma, J. P.; Gertner, B. J.; Wilson, K. R.; Hynes, J. T. *J. Chem. Phys.* **1987**, *86*, 1356.

(34) Gertner, B. J.; Wilson, K. R.; Hynes, J. T. *J. Chem. Phys.* **1989**, *90*, 3537.

(35) Amovilli, C.; Mennucci, B.; Floris, F. M. *J. Chem. Phys.* **1998**, *102*, 3023.

(36) Han, C.-C.; Dodd, J. A.; Braumann, J. I. *J. Phys. Chem.* **1986**, *90*, 471.

(37) Lyubartsev, A. P.; Laaksonen, A. *J. Phys. Chem.* **1996**, *100*, 16410.

(38) Allen, M. P.; Tildsley, D. J. *Computer Simulation of Liquids*; Clarendon: Oxford, U.K., 1987.

(39) Vande Linde, S. R.; Hase, W. L. *J. Chem. Phys.* **1990**, *93*, 7962.

(40) Vande Linde, S. R.; Hase, W. L. *J. Phys. Chem.* **1990**, *94*, 2778.

(41) Frisch, M. J.; Trucks, G. W.; Schlegel, H. B.; Gill, P. M. W.; Johnson, B. G.; Robb, M. A.; Cheeseman, J. R.; Keith, T.; Petersson, G. A.; Montgomery, J. A.; Raghavachari, K.; Al-Laham, M. A.; Zakrzewski, V. G.; Ortiz, J. V.; Foresman, J. B.; Cioslowski, J.; Stefanov, B. B.; Nanayakkara, A.; Challacombe, M.; Peng, C. Y.; Ayala, P. Y.; Chen, W.; Wong, M. W.; Andres, J. L.; Replogle, E. S.; Gomperts, R.; Martin, R. L.; Fox, D. J.; Binkley, J. S.; Defrees, D. J.; Baker, J.; Stewart, J. P.; Head-Gordon, M.; Gonzalez, C.; Pople, J. A. *Gaussian 94*; Gaussian, Inc.: Pittsburgh, PA, 1995.

(42) Helgaker, T.; Jensen, H. J. Aa.; Jörgensen, P.; Olsen, J.; Ruud, K.; Ågren, H.; Andersen, T.; Bak, K. L.; Bakken, V.; Christiansen, O.; Dahle, P.; Dalskov, E. K.; Enevoldsen, T.; Fernandez, B.; Heiberg, H.; Hettema, H.; Jonsson, D.; Kirpekar, S.; Kobayashi, R.; Koch, H.; Mikkelsen, K. V.; Norman, P.; Packer, M. J.; Saue, T.; Taylor, P. R.; Vahtras, O. *Dalton, An electronic structure program*, release 1.0 (1997); see http://www.kjemi.uio.no/software/dalton/dalton.html.

(43) Shaik, S. S.; Schlegel, H. B.; Wolfe, S. *Theoretical Aspects of Physical Organic Chemistry − The S_N2 Mechanism*; John Wiley & Sons, Inc.: New York, 1992.

(44) Cossi, M.; Adamo, C.; Barone, V. *Chem. Phys. Lett.* **1998**, *287*, 1.

(45) Larson, J. W.; McMhon, T. B. *J. Am. Chem. Soc.* **1985**, *107*, 766.

(46) Albery, W. J.; Krevoy, M. M. *Adv. Phys. Org. Chem.* **1978**, *16*, 87.

(47) Kalhori, S.; Elander, N.; Svennebrink, J.; Stone-Elander, S. Manuscript Department of Physics, Stockholm University, Stockholm, Sweden, 2001.

(48) Jackson, J. D. *Classical Electrodynamics*, 3rd ed; John Wiley and Sons: New York, 1998.

(49) Ensing, B.; Meijer, E. J.; Blöchl, P. E.; Baerends, E. J. *J. Phys. Chem. A* **2001**, *105*, 3300.

(50) Mohamed, A. A.; Jensen, F. *J. Phys. Chem. A* **2001**, *105*, 3259.

(51) Tucker, S. C.; Truhlar, D. G. *J. Am. Chem. Soc.* **1990**, *112*, 3347.

(52) The Molden code is described at and can be obtained from: http://www.cmbi.kun.nl/∼ schaft/molden/molden.html.